HARVEY W. KO, HOWARD S. BURKOM, JOSEPH P. SKURA, and DURVIS A. ROBERTS

AN ANALYSIS OF EMPE CODE PERFORMANCE IN A SELECTION OF LATERALLY INHOMOGENEOUS ATMOSPHERIC-DUCT ENVIRONMENTS

Articles in an earlier issue of this publication introduced the methodology for APL's Electromagnetic Parabolic Equation (EMPE) code, discussed the code's advantages over other models, and showed its agreement with some data. In this article, EMPE predictions are compared with those of the established theoretical coupled-mode model of Cho and Wait and with a variety of field test data. Together, these examinations show that the EMPE code can describe electromagnetic wave propagation loss in range-dependent atmospheric-duct environments.

INTRODUCTION

The Electromagnetic Parabolic Equation (EMPE) code is a physical optics code that calculates electromagnetic propagation loss through all types of anomalous refractive atmospheres for antennas radiating over a smooth surface. Its value stems from its computational efficiency; it quickly supplies answers for propagation loss and antenna coverage, including elevated-duct and various range-dependent refractive situations. Previously, solutions by other computational methods, such as the coupled-mode approach, restricted cases to simply characterized surface or evaporative ducts. For those methods, computer-based calculations for laterally inhomogeneous, i.e., range-dependent, refractive conditions are generally prohibitive, taking hours of computer processing time. EMPE, on the other hand, provides solutions in minutes for laterally inhomogeneous, vertically complex atmospheres, often with several types of vertical refractive changes (i.e., ducting, superrefraction, and subrefraction) at each range.

Since its introduction in 1983,[1] the EMPE code has been valuable in describing the performance of radiating electromagnetic systems in several anomalous propagation circumstances investigated at APL,[2,3] and has provided the basis for radar coverage predictions at radar sites worldwide.[4] In addition, it has been successfully used to estimate incident surface power and radar clutter under surface ducting conditions (see the article by Lee et al. elsewhere in this issue), excess fade loss in communications systems,[5] and errors in aircraft microwave landing systems.

Confidence in EMPE calculations stems from APL's field experiments[2,3] and from comparisons between EMPE solutions and results of other investigations. In this article, EMPE results are compared with results from the coupled-mode model of Cho and Wait,[6] which is considered by most as the theoretical gauge for new model calculations pertaining to a laterally inhomogeneous environment. We also survey the results of several studies at APL that compare EMPE predictions for horizontally polarized waves over a smooth, infinitely conducting surface with well-accepted field test data taken as early as 1944. Those venerable datasets came from the most extensively cited over-water measurements for microwave propagation loss in ducting environments. Because of their open distribution and expansive test geometries, the datasets are commonly used as empirical gauges for new model calculations.

TROPOSPHERIC-DUCT PROFILES

The existence of anomalous refractive layers in the atmosphere can be determined by calculating the radio index of refraction, n, or, equivalently, the modified refractivity, M, where $M = (n - 1) \times 10^6 + 0.157z$, and z is height in meters, from measured values of temperature, pressure, and humidity.[1] The types of propagation present in any layer are given in Table 1. Figure 1 shows three stylized M profiles for conditions in the

Table 1—Types of propagation.

Type	M gradient, dM/dz (km^{-1})
Trapping	≤ 0 (anomalous)
Superrefractive	0 to 78 (anomalous)
Standard	78 to 157
Subrefractive	> 157 (anomalous)

evaporation duct, the elevated duct, and the surface-based elevated duct that may trap or duct microwave rays in the surface-based regions, defined by $z < D$, and the elevated regions, defined by $(z_2 - \tau) < z < z_2$. Two inflection points, z_1 and z_2, are shown for the elevated-duct type. The first inflection point, z_1, is called the optimum coupling height (OCH).
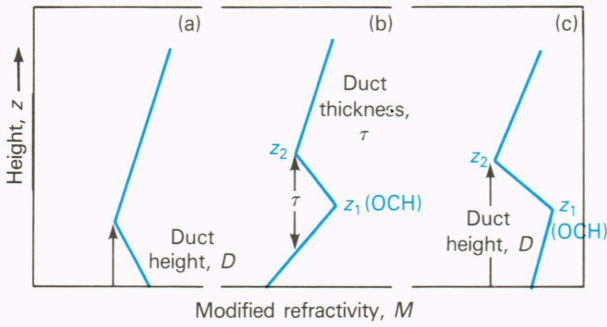
Figure 1—Stylized vertical profiles of modified refractivity, M, for (a) the evaporation duct, (b) the elevated duct, and (c) the surface-based elevated duct. OCH = optimum coupling height, z_1.

THE PARABOLIC APPROXIMATION FOR PROPAGATION IN INHOMOGENEOUS MEDIA

When inhomogeneities in the dielectric constant are considered as varying in both the vertical and horizontal directions, Maxwell's equations for propagation in the troposphere are generally nonseparable and difficult to solve analytically. Cho and Wait[6] have approached the problem numerically by means of coupled-mode analysis, using a cylindrical-earth model and an infinite line source; horizontal inhomogeneities are considered by assuming horizontally piecewise-uniform media. The advantage of their formulation is that the electromagnetic field within each piecewise-uniform section can be represented by a discrete sum of modes. Mode conversion at the junction between two sections is obtained by invoking mode orthogonality and continuity of electric and magnetic fields. Modal analysis tends to be difficult with computer cost limiting convergent answers to simple refractive environments.

A well-known approximation, the parabolic approximation, was obtained in 1946 by Fock[7] for propagation in a vertically inhomogeneous, horizontally homogeneous atmosphere over a spherical earth. The EMPE code extends the spherical-geometry approach to include both horizontal and vertical inhomogeneities. These variations are represented by treating the atmospheric dielectric constant ϵ as a function of the distance r measured from the center of the earth, and of the polar angle θ, but not of the azimuthal angle ϕ, so that $\epsilon = \epsilon(r,\theta)$. Thus, ϵ is assumed to behave identically in all vertical planes of propagation. If azimuthal independence is assumed, the variations in the atmospheric dielectric constant are limited to two dimensions, greatly simplifying the mathematics. Also for mathematical simplification, the source field is assumed to originate from a raised vertical electric dipole (VED) at the pole. The resulting approximate equation governing propagation, however, will be the same if a vertical magnetic dipole (VMD) source is assumed; only the boundary conditions to be satisfied at the earth's surface will differ.

We now present the highlights of the derivation of the EMPE equation.[1] With the usual assumption of a constant magnetic permeability μ in the atmosphere, Maxwell's equations may be combined to eliminate the electric field $\mathbf{E}$ and to obtain

$$\nabla \times \nabla \times \mathbf{H} + \omega^2 \mu\epsilon\mathbf{H} = -\frac{\nabla\epsilon}{\epsilon} \times (\nabla \times \mathbf{H}),$$

(1)

where ω is the signal frequency in rad/s. Given the assumed symmetries and the VED source, only the components E_r, E_θ, and H_ϕ do not vanish. Therefore, the magnetic field $\mathbf{H}$ may be written $\mathbf{H} = H(r,\theta)\mathbf{l}_\phi$ and is completely determined by the scalar function $H(r,\theta)$. This expression for $\mathbf{H}$ is substituted into Eq. 1 to obtain a single scalar differential equation. Generally, one is interested in examining variations in the fields that are long compared with a wavelength. It is expected that, along the earth's surface in the horizontal direction from the source, the fields will oscillate in a manner described by e^{iks} (s is the range and the wave number, k, equals $2\pi/\lambda$, where λ is the signal wavelength). A convenient substitution that factors out rapidly oscillating behavior, as well as large variations near the source (a linear trend in radius), is obtained in terms of an attenuation function $U(r,\theta)$, defined by

$$H(r,\theta) = \frac{U(r,\theta)}{r} (\sin\theta)^{-\frac{1}{2}} \epsilon^{-1} e^{ik_0 a\theta}.$$

(2)

Here, $k_0^2 = \omega^2\mu\epsilon(a,0) = \omega^2\mu\epsilon_0$ is the square of the electromagnetic wave number just above the earth's surface, $r = a$.

The scalarized version of equation (Eq. 1) is combined with Eq. 2 to obtain a propagation equation for $U(r,\theta)$, an elliptic differential equation in r and θ. That equation is transformed from the spherical coordinate variables r and θ to the measured quantities z and s, where z is the altitude above the earth's surface and s is the arc length along the surface—essentially the downrange distance from the antenna. The transformation is simply $z = r - a$, $s = a\theta$, where a is the earth's radius. The next step is to drop some relatively insignificant terms and to invoke the fundamental premises of Leontovich and Fock concerning the growth of U. Then $U(z,s)$ is given, to good approximation, by

$$\frac{\partial^2 U}{\partial z^2} + 2ik_0 \frac{\partial U}{\partial s}$$

$$+ k_0^2 \left[\frac{\epsilon(z,s) - \epsilon_0}{\epsilon_0} + \frac{2z}{a}\right] U = 0.$$

(3)

Equation 3 is a parabolic differential equation that is second order in the vertical direction and first order in the horizontal direction. The effects of the atmospheric inhomogeneities are contained in $\epsilon(z,s)$. The expression $2z/a$ in the third term represents the effect of the earth's curvature. In the EMPE code, the expression $(\Delta\epsilon/\epsilon_0 + 2z/a)$ is stored, in effect, as modified refrac-

90

tivity at each range, thus allowing EMPE to work in height–range space while including the diffraction that is caused by a spherical earth.

The conditions that must be satisfied so that the original elliptic equation may be approximated by the parabolic Eq. 3 are summarized as follows:

(a) $\dfrac{1}{\epsilon}\left|\dfrac{\partial\epsilon}{\partial s}\right| \stackrel{<}{\sim} 10^{-4}k_0$,

(b) $\theta > 10^2(k_0 a)^{-1}$, $\quad s > 10^2/k_0$

(c) $k_0 a\left|\dfrac{\partial U}{\partial\theta}\right| >> \dfrac{\partial^2 U}{\partial\theta^2}$,

$k_0\left|\dfrac{\partial U}{\partial s}\right| >> \dfrac{\partial^2 U}{\partial s^2}$

(d) $\dfrac{1}{\epsilon}\dfrac{\partial\epsilon}{\partial z} << \left(\dfrac{2k_0^2}{a}\right)^{1/3}$.

If one associates $\epsilon|\partial\epsilon/\partial s|^{-1}$ and $\epsilon|\partial\epsilon/\partial z|^{-1}$ with the radii of curvature of rays resulting from horizontal and vertical variations in ϵ, then conditions (a) and (d) require that those radii be large compared with a wavelength; that is, the horizontal and vertical variations in ϵ must be reasonably slow. For situations of interest here, that requirement holds. Condition (b) implies that reasonable values will be obtained for distances greater than 16 wavelengths from the source. Finally, condition (c) requires that the propagation be relatively oblique—that is, that rays be launched with low grazing angles ($\lesssim 20°$).

Solutions to the parabolic equation will be obtained if the initial source field is specified and if the values of the field at the earth's surface and at the upper-atmosphere limit are properly defined. For simplicity, a nonreflecting or fully absorbing boundary is assumed at the upper limit. For the surface boundary conditions, a smooth-surfaced, conducting earth is assumed; it is also reasonable to assume that the skin depth of radiation within the earth is small compared with the earth's radius of curvature. Under that assumption, the boundary effect of the earth's curvature can be ignored, and Leontovich's impedance boundary condition[8] can be applied. If η_s is the complex dielectric constant of the earth, the boundary condition on $U(z,s)$ will be satisfied for a VED if

$$\dfrac{\partial U}{\partial z} + \dfrac{ik}{\sqrt{\eta_s}}U = 0 \quad \text{at } z = 0 . \qquad (4)$$

For a VMD source, the boundary condition on $U(z,s)$ will be

$$\dfrac{\partial U}{\partial z} + ik\sqrt{\eta_s}\, U = 0 \quad \text{at } z = 0 . \qquad (5)$$

Practically speaking, vertical symmetric and antisymmetric solutions for U about the surface must be combined to satisfy either Eq. 4 or Eq. 5. If the earth's surface is approximated by a perfect conductor, however, Eqs. 4 and 5 reduce to the requirement that either $\partial U/\partial z = 0$ (VED) or $U = 0$ (VMD) at the surface. In those cases, only vertical solutions that are symmetric (VED) or antisymmetric (VMD) about the surface need to be obtained, and the boundary conditions are automatically satisfied.

COMPARISON OF EMPE WITH A COUPLED-MODE MODEL

Cho and Wait[6] use a stylized, trilinear, elevated-duct profile (Fig. 1b) as the basis for creating a horizontally inhomogeneous environment to obtain numerical examples for their coupled-mode approach. The optimum coupling height (OCH) is initially 600 m; the trapping layer gradient strength used by Cho and Wait is extremely large, since a nearly horizontal jump of 25 units in M represents the layer. We use a gradient strength of -2.5×10^6 km^{-1}, and the standard gradient strength above and below the trapping layer is 117 km^{-1}. Interestingly, there would never be a real atmospheric environment with such a strong elevated-duct gradient, but this example is well known as a test case, and it allows direct model comparisons. In case c in Fig. 2, the OCH is held constant from the antenna to 200 km downrange, then raised 40 m every 30-km step thereafter until reaching 500 km downrange, where it attains a height of 1000 m. The OCH is lowered by 40 m every 30-km step until reaching 800 km downrange and then held at 600 m from 800 to 1000 km downrange. In all, 21 lateral changes are made.

In case c, a transmitter frequency of 200 MHz is used for an antenna at 600-m elevation, which is the OCH at zero range. Figure 3 compares Cho and Wait's case c prediction (black) with EMPE predictions. The first EMPE calculation (blue) results from using the same 21 horizontally uniform slabs (see Fig. 2) as for the Cho and Wait calculation. Lateral changes in refractivity occur every 30 km. The EMPE losses agree well with the Cho and Wait losses, especially at the more distant ranges. Differences appear in some of the fine structure, which is reasonable considering the different analytical methods.
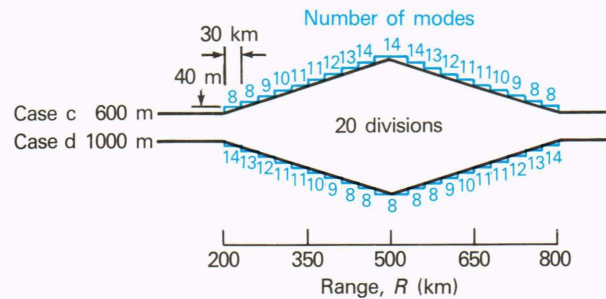

Figure 2—Two laterally inhomogeneous cases used by Cho and Wait to describe the range dependence of the OCH of an elevated duct.
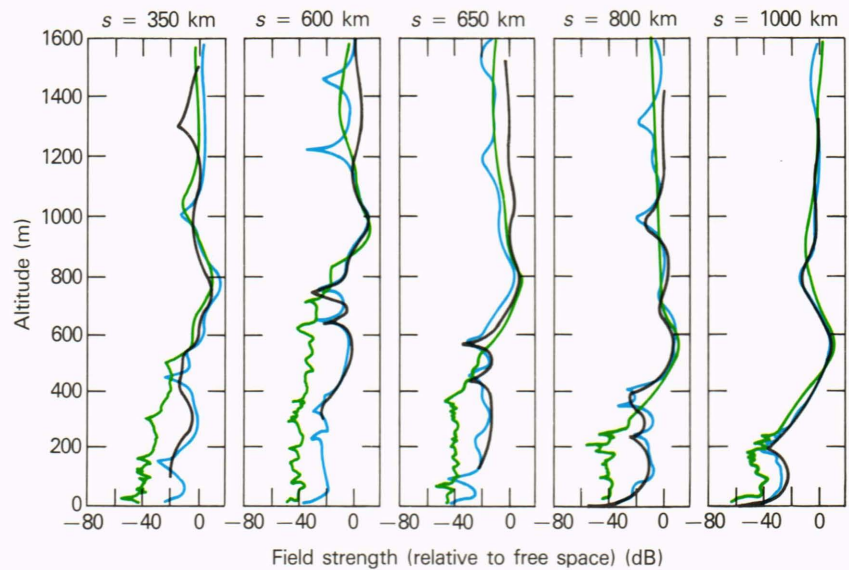
Figure 3—A comparison of the Cho and Wait results for case c (black) with EMPE results using 20 range steps (blue) and over 1600 range steps (green). Frequency = 200 MHz.

In the second EMPE calculation (green), a linear interpolation is used between the range steps prescribed in Fig. 2. A new lateral refractive change is inserted every 0.37 km, giving a total of over 1600 lateral changes along the path. As expected, the interpolation causes no significant propagation loss changes above the duct. Below the duct the propagation loss changes by an average of more than 10 dB if the interpolation is made. In the original Cho and Wait study, although the number of included modes is probably adequate, the exchange of energy among these modes is not well modeled if the 30-km slabs are used. In the second EMPE result, the increased modal interaction explains the 10-dB average difference. In another study,[9] using the same type of normal-mode model and the same refractivity environment, the number of slabs was chosen carefully to give convergent results; the slab size required was about 5 km. That computational experiment suggests that the interpolation is necessary to compute transmission loss accurately when the refractivity profiles display strong range-dependent features. From a practical aspect, the run time added by the EMPE interpolation feature is insignificant computationally. The coupled-mode result requires hundreds of computer processing minutes. The first EMPE result without interpolation required 467 s, and the second EMPE result with interpolation required 642 s.

Figure 4 shows results for the comparison of EMPE with the Cho and Wait case d (see Fig. 2), where the environment is inverted, in the sense that the OCH drops from 1000 to 600 m and returns to 1000 m as the path is traversed. Here, a 200-MHz antenna is placed at 1000-m altitude. Again, the EMPE results are shown without interpolation (blue) and with interpolation (green).

ELEVATED DUCTING
OFF SAN DIEGO IN 1944

Figure 5 compares EMPE predictions with measurements under atmospheric conditions described by a close-range elevated duct and a downrange surface-evaporative duct. In 1944, the Naval Electronics Laboratory (NEL) (now the Naval Ocean Systems Center) performed vertical soundings off the coast of San Diego.[10] Land-based transmitters at 30.5-m elevation radiated at frequencies (wavelengths) of 63 MHz (4.8 m), 167 MHz (1.8 m), 526 MHz (57 cm), and 3.3 GHz (9 cm). The radar horizon was 19.4 km. Vertical profiles of modified refractive index M and field strength (in dB relative to free space) are shown in Fig. 5 from the surface up to 1.5-km altitude. At 19-km range, an elevated duct is measured. At 130-km range, the main feature has changed to a surface-based elevated duct. At 186-km range, the refractive profile is that of a surface-evaporative duct.

To implement an EMPE prediction, a linear interpolation in modified refractivity is made for ranges between the ranges where refractivity was measured. The close-range M profile is used for all ranges between its measurement range and the antenna, and the far-range M profile is used for all ranges beyond its measurement range. At 526 MHz, the EMPE results (red curve) agree with the measured data (black curve) in and below the duct at all ranges. The differences above the duct in the measured data are caused by horizontal meteorological variations in duct height and strength that are more volatile in range than the scale shown by the three profiles used in the EMPE calculations. At 167 MHz, the comparison is not as favorable, especially at the larger ranges of 178 and 232 km. At the longer wavelength, the trapping ability of the duct is marginal, and even minor changes in the duct strength and height can have a pronounced effect on the trapping.

Much better results are obtained by comparing EMPE predictions with data for a slowly changing elevated-duct environment, also measured by NEL off San Diego in 1944. There, an elevated duct was measured (Fig. 6) at ranges of 19, 94, and 186 km. The figure shows the elevated duct slowly rising at each downrange position.
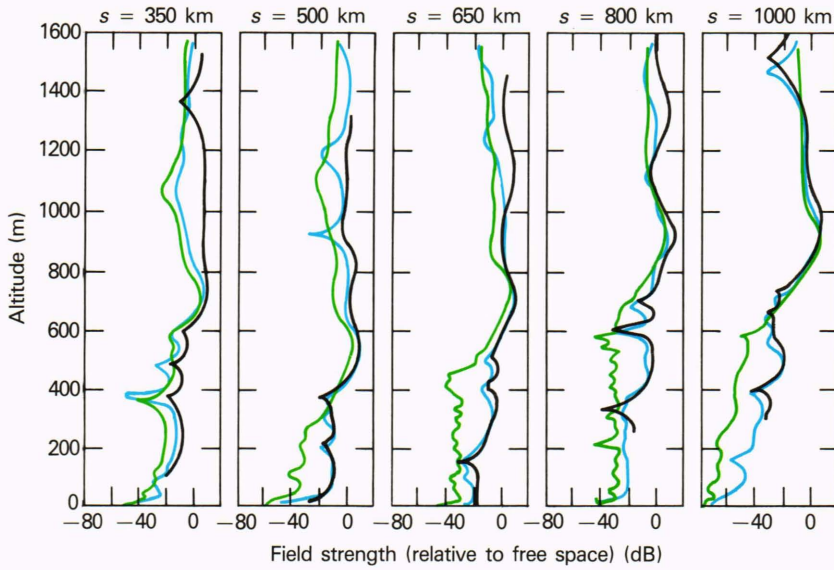
Figure 4—A comparison of the Cho and Wait results for case d (black) with EMPE results using 20 range steps (blue) and over 1600 range steps (green). Frequency = 200 MHz.
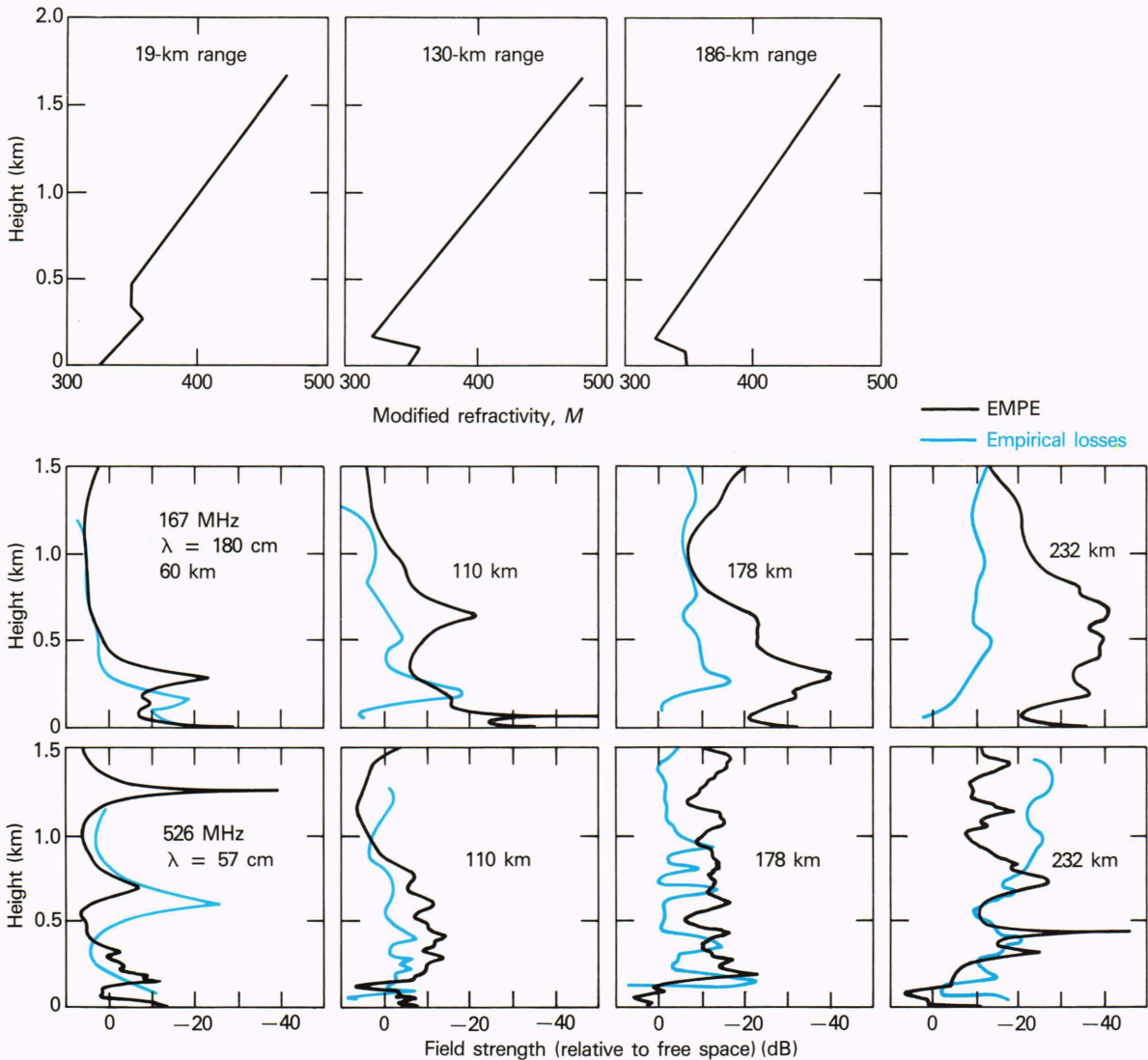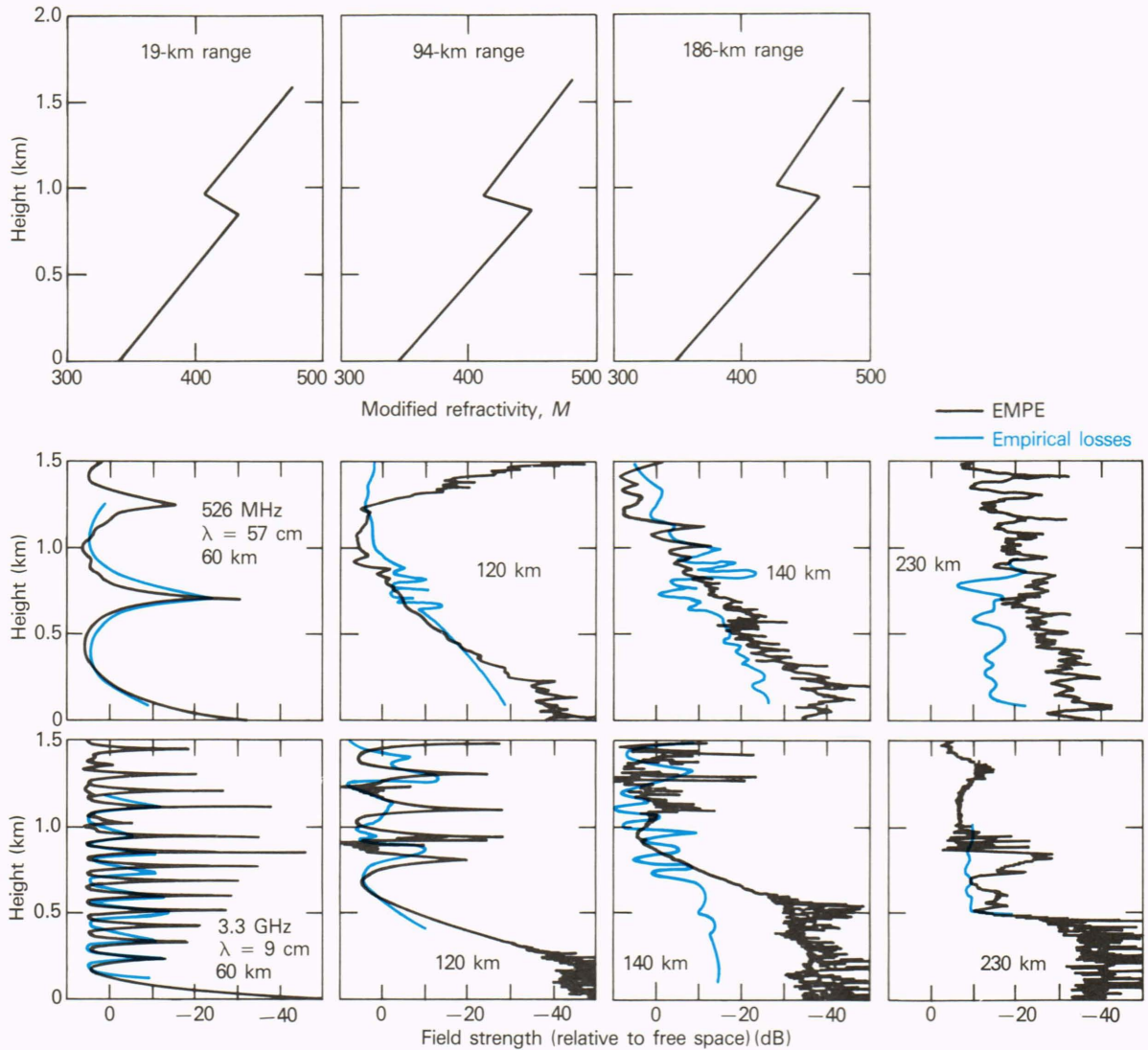

Figure 5—Vertical profiles for the modified refractive index, measured field strength, and EMPE calculations at various ranges for measurements off San Diego on 2 October 1944. The refractive environment changes from an elevated duct near the coastline at 19-km range to a surface-evaporative duct at 186-km range.

Figure 6—Vertical profiles for the modified refractive index, measured field strength, and EMPE calculations at various ranges for measurements off San Diego on 29 September 1944. A laterally changing elevated duct is measured at all ranges.

The same refractivity interpolation procedure used to obtain the data in Fig. 5 was used here. EMPE results (red line) agree well with the data (black line) at most ranges for the frequencies of 526 MHz and 3.3 GHz.

SURFACE-EVAPORATIVE DUCTING NEAR ANTIGUA IN 1945

In the spring of 1945, an extensive series of propagation-loss measurements in the surface-evaporative duct environment was performed by the Naval Research Laboratory at Antigua, British West Indies. Frequencies of 10 and 3.3 GHz (wavelengths of 3 and 9 cm) were emitted by transmitters at 5 and 14 m, respectively, on a tower at the water's edge.[11] If the reported M profile with a duct height of about 15 m is considered horizontally homogeneous, a resultant EMPE coverage diagram shows the 10-GHz energy clearly trapped and ducted to great range (R) in the duct. The data for the duct, how-

ever, showed a one-way falloff rate less rapid than standard (i.e., $1/R^2$, where R is the horizontal range) but not as rigid as that predicted by theory for a horizontally homogeneous surface duct (i.e., $1/R$); these data were enigmatic to analysts[12] for many years. The EMPE code's ability to analyze falloff rate in the horizontally inhomogeneous environment allows us to speculate on the nature of these data.

The following refractivity scheme was input to EMPE in an attempt to model the horizontal changes in the experiment described above: The original surface-duct height was allowed to diminish at a rate of 0.08 km^{-1} out to a range of 85 km, beyond which it was held constant at a height of 9 m. The surface M value was reduced at a rate of 0.09 km^{-1} out to 280 km in accordance with our boundary-layer modeling procedures reported earlier.[1,2] The progressively weaker duct caused energy to be trapped near the transmitting antenna and allowed duct leakage to occur downrange.

94

EMPE results are compared with the measured Antigua data at 10 GHz in Fig. 7. The data, taken on eight days from the 5-m transmitter to a 4-m receiver, are shown in red on the figure. The difference in falloff rates computed by EMPE is shown for homogeneous and inhomogeneous ducting conditions; the free-space falloff rate is also shown. At ranges out to 93 km, both duct types lead to EMPE results that agree with the data. Beyond 93 km the EMPE result for the inhomogeneous duct shows distinctly better agreement than the homogeneous duct result. Data for 3-GHz measurements are shown in Fig. 8 for the 14-m transmitter and a 29-m receiver. Again, the EMPE result for the inhomogeneous duct model derived from the original M profile gives the better agreement. Figures 7 and 8 demonstrate the importance of inhomogeneous duct modeling when analyzing actual ducting situations. They show the necessity for detailed meteorological measurements at several ranges when scientific analysis is required for propagation-loss investigations.

ELEVATED AND SURFACE-BASED ELEVATED DUCTS OFF GUADALUPE ISLAND IN 1947 AND 1948

The most extensive radio-meteorological data set ever reported was gathered by NEL from 1945 to 1948. Data were obtained along a 520-km overwater path between Guadalupe Island and San Diego.[13] A PBY aircraft, equipped with radio transmitters and temperature sensors, flew a vertical sawtooth pattern from near the surface to 1200-m altitude. Transmitters on the airplane radiated at 63, 170, 520, and 3300 MHz. Receiving antennas were located at San Diego at 30.5- and 150-m heights. Measurement of air temperature and dew point by the airplane permitted the calculation of profiles.[14] Figure 9, a sample output from the 150-m antenna, displays the meteorological profiles given in B-type refractive units ($B = M - 0.118\,h$, where h is the height in meters) and also profiles of propagation loss in decibels relative to free space for the four frequencies at various ranges.

The data from this experiment were analyzed with the EMPE code, using different sets of refractivity profiles, all derived from the same meteorological data. The difference between the sets is either the number of data points included in each profile or the number of profiles used (i.e., one horizontally homogeneous environment in some cases). On 12 March 1948 (Fig. 9), a laterally inhomogeneous eleveated duct was measured. The raw meteorological data show a surface-based elevated duct at 74 km changing to a rising elevated duct at 148 km, then rising again and evolving into an elevated super-refractive layer beyond 372 km. Table 2 summarizes the environment. The receiver antenna height was 30.5 m. The elevated ducting environment gave energy well beyond the geometrical horizon and at power levels above free-space loss.

Figure 10 summarizes the 12 March 1948 results for 170 MHz. Vertical propagation-loss data in decibels relative to free space are shown for ranges of 148, 222, and
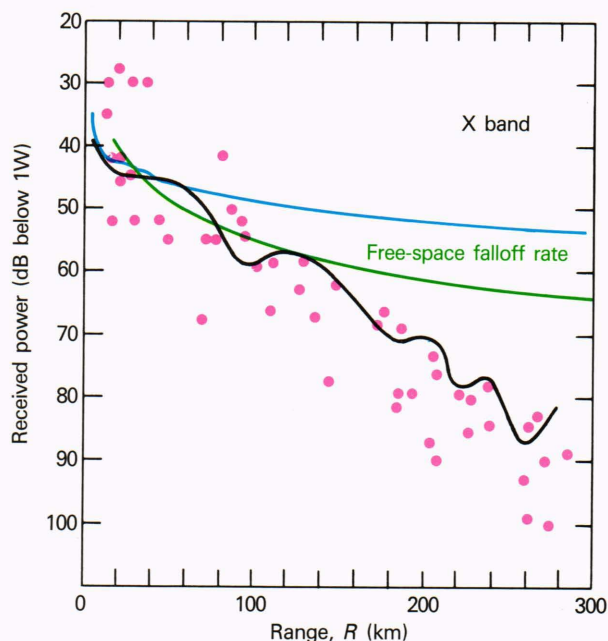
Figure 7—Comparison of evaporation-duct signal falloff data (red) at 3-cm wavelength, measured near Antigua in 1945, with EMPE calculations for homogeneous (blue) and inhomogeneous (black) ducting conditions extrapolated from a single modified-refractivity profile measurement.
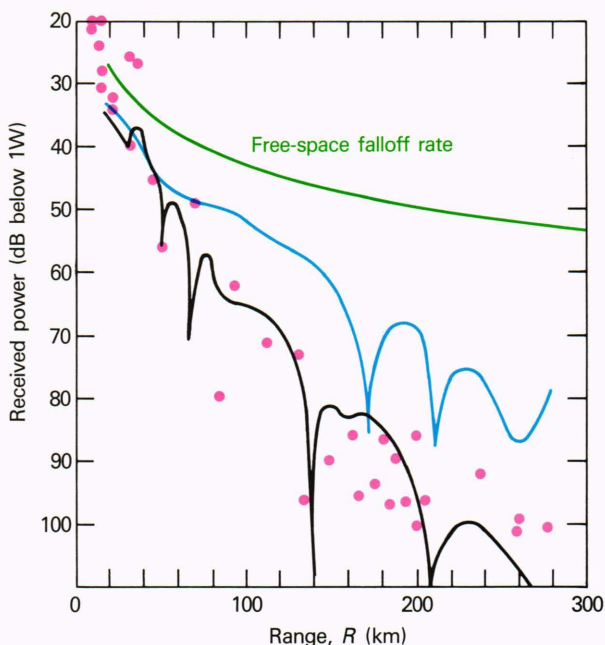
Figure 8—Comparison of evaporation-duct signal falloff data (red) at 9-cm wavelength, measured near Antigua in 1945, with EMPE calculations for homogeneous (blue) and inhomogeneous (black) ducting conditions extrapolated from a single modified-refractivity profile measurement.

297 km. These losses are plotted with losses computed by mode conversion and WKB methods.[9] The mode-conversion method uses normal mode theory to compute losses at each range. The modal sums are adjusted for
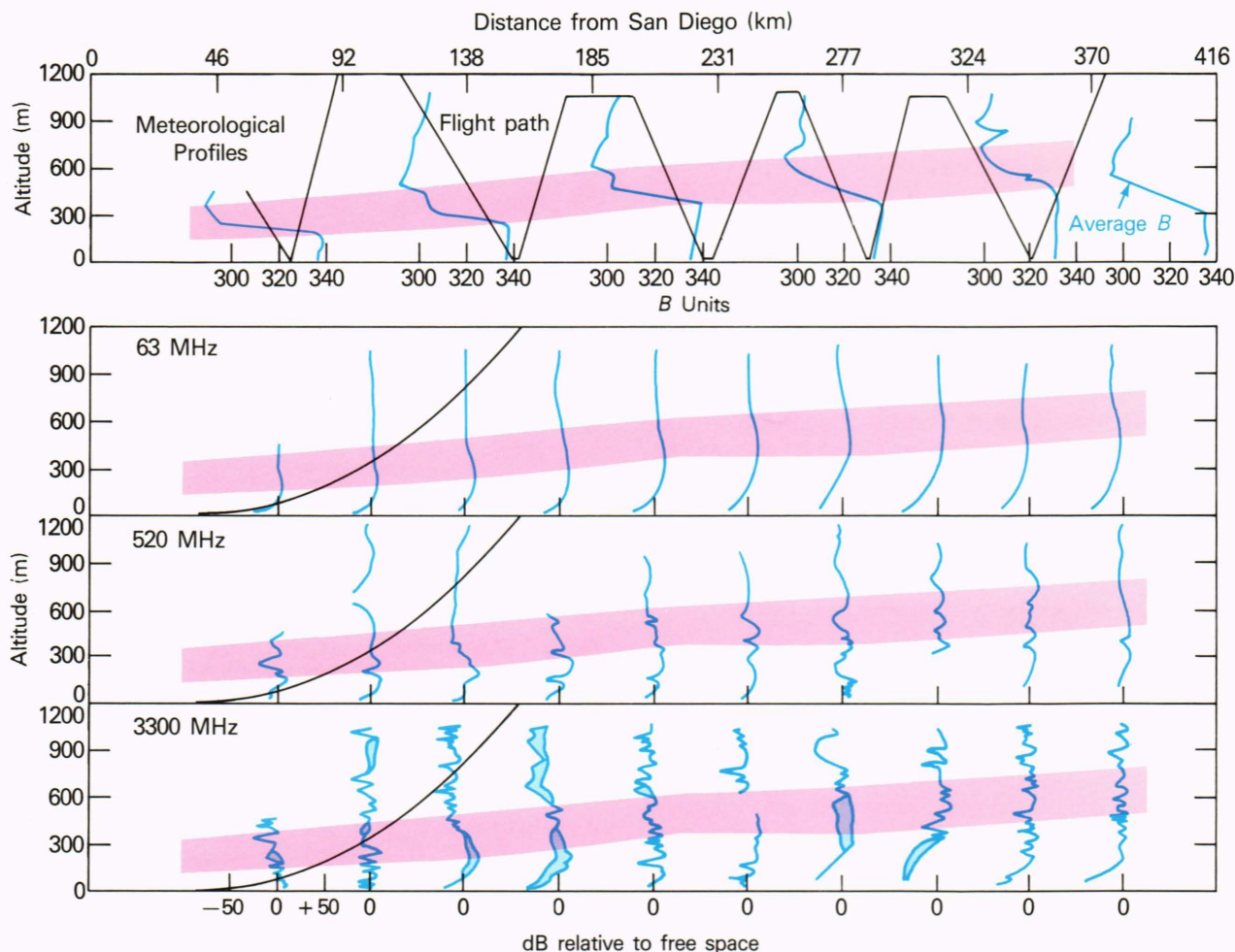
Figure 9—Guadalupe Island data taken on 12 March 1948. Receiver height is 150 m (reproduced by permission, H. Hitney, Naval Ocean Systems Center, San Diego).

Table 2—Range-dependent, anomalous refractive conditions measured on 12 March 1948.

Range (km)	Anomalous Propagation Type	Approximate Altitude (m)
0–74	Surface-based elevated duct	0–335
148	Elevated duct	150–460
223	Elevated duct	300–610
298	Elevated duct	300–610
372	Elevated superrefractive	460–730

downrange energy transfer between modes, using a set of conversion coefficients that are updated when the refractivity profile changes. The WKB or adiabatic method also uses modal decomposition at each range. However, this method adjusts the modal eigenangles along the propagation path by range-averaging them separately for each mode. EMPE results are shown for instances when the refractivity profiles are described by (1) an average profile used at all ranges (horizontally homogeneous); (2) range-dependent profiles (horizontally inhomogeneous;

mogeneous), each described by four data points per profile; and (3) range-dependent profiles (horizontally inhomogeneous), each described by six data points per profile. Clearly, EMPE results with the horizontally homogeneous, average elevated-duct profiles do not give favorable comparisons with the data. EMPE results with either the four- or six-point profiles yield more favorable comparisons. The six-point profiles preserve the vertical fine structure, and, in some instances for 170-MHz, the EMPE results look better than results from the other analytical methods.

Experimental controls probably did not allow the pointing or elevation angles of the transmitter antennas to be held rigid, and it is difficult to determine the accuracy in measuring propagation loss. Further, the ranges at which the propagation loss is reported must be average ranges because of the transmitter sawtooth flight. Therefore, although the Guadalupe data are the most extensive available, any comparisons are qualitative at best.

Computational analysis of the Guadalupe data by other investigators has been limited to the lower frequencies because of the tremendous computational constraints posed by modal or WKB methods. EMPE computational effi-
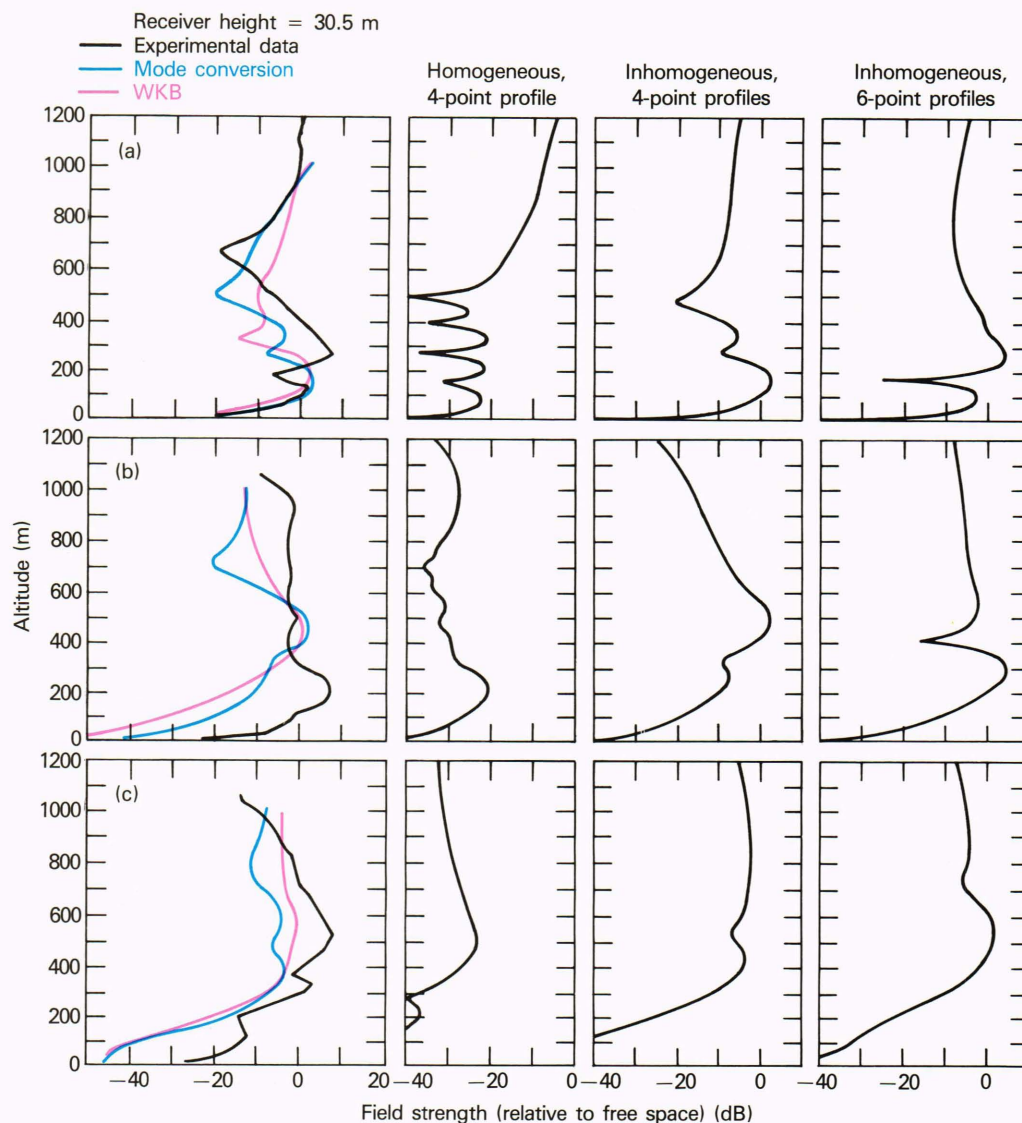
Figure 10—Propagation-loss data and EMPE results for 170-MHz measurements on 12 March 1948 between Guadalupe Island and San Diego. Vertical profiles of loss in decibels relative to free space are given at ranges of (a) 148, (b) 222, and (c) 297 km from the transmitter.

ciency has allowed analysis of nearly all the Guadalupe data. Figure 11 shows additional EMPE results for the 12 March 1948 measurement at (a) 65 MHz at 335-km range, (b) 520 MHz at 335-km range, and (c) 3300 MHz at 298-km range. Refractivity profiles used for Fig. 11 incorporate over 10 data points per range-dependent profile, retaining almost all the meteorological data for the laterally inhomogeneous condition.

On 8 April 1948, the Guadalupe Island measurements showed excess energy trapped in a laterally inhomogeneous, surface-based elevated duct. Again, using range-dependent refractivity profiles that retained almost all the vertical variations measured, good agreement with the data was obtained using EMPE (see Fig. 12 for 170 MHz at ranges of 298 and 484 km).

ELEVATED DUCTS NEAR HAWAII IN 1977

Airborne transmitters and airborne receivers were used near Hawaii from 16 May through 24 June 1977 to study elevated ducting.[15] These experiments have provided the best radio-meteorological data for elevated-ducting analysis with both transmitters and receivers at altitudes in or near the duct. Frequencies of 150, 450, and 2200 MHz were used. Measurements were made along an overwater, 510-km path between the islands of Hawaii and Kauai. A UH-3 helicopter equipped with beacon receivers and meteorological instruments to measure temperature, pressure, and humidity was flying off the Kauai coast. A U-21 airplane equipped with beacon receivers
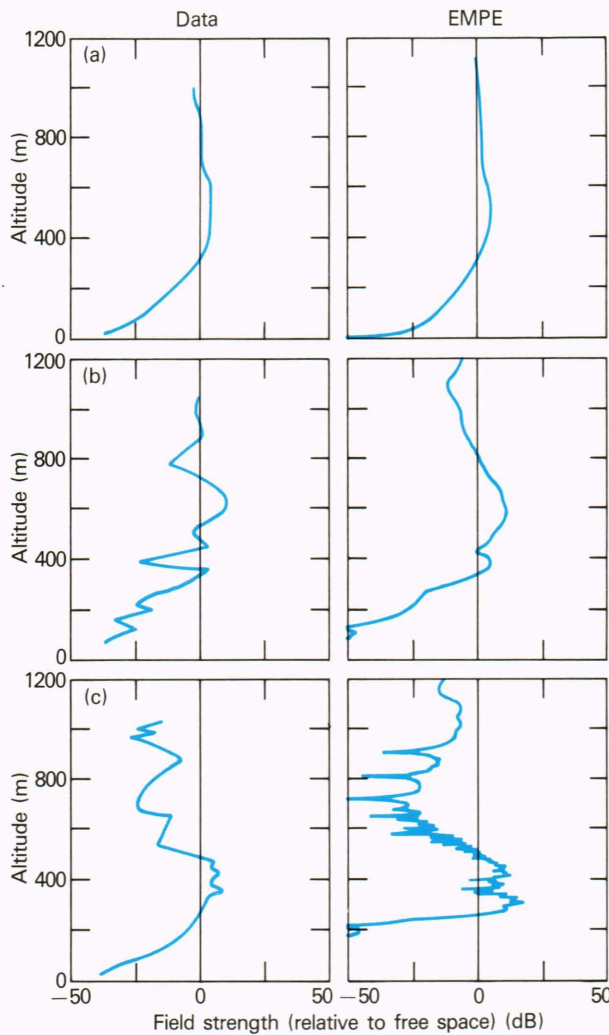
Figure 11—EMPE comparison with data from 12 March 1948, taken off Guadalupe Island at (a) 65 MHz, 335-km range; (b) 520 MHz, 335-km range; and (c) 3300 MHz, 298-km range.

Figure 12—EMPE comparison with data from 8 April 1948, taken off Guadalupe Island at 170 MHz for (a) 298-km range and (b) 484-km range. Antenna height is 152.4 m.

Figure 13—Modified refractivity profiles obtained off Hawaii on 22 June 1977 (reproduced by permission, D. Woods).

and similar meteorological instruments flew a vertical sawtooth path from Kauai to Hawaii. At South Point, Hawaii, a UH-1 helicopter transmitted signals as it flew at the altitude of the elevated duct, typically between 1000 and 2000 m.

Figure 13 shows the modified refractivity profiles obtained by measurements on board the UH-3 and U-21 aircraft. A horizontally inhomogeneous, elevated-duct atmosphere existed generally between altitudes of 900 and 1500 m with -160 km^{-1} gradient strength. The transmitter on the UH-1 helicopter was stationed just above the duct at 1554 m.

Figure 14a shows the EMPE coverage diagram predicted for the 2.2-GHz antenna in a horizontally homogeneous, elevated-duct environment given by the average duct features. The color scale maps the one-way propagation loss. The warmer colored areas indicate the higher-energy regions; the cooler colored areas are the lesser-energy regions. Little energy is seen below the elevated duct, located between 1000 and 2000 m. Beyond 350 km, energy is confined within the elevated duct, with upward leak-
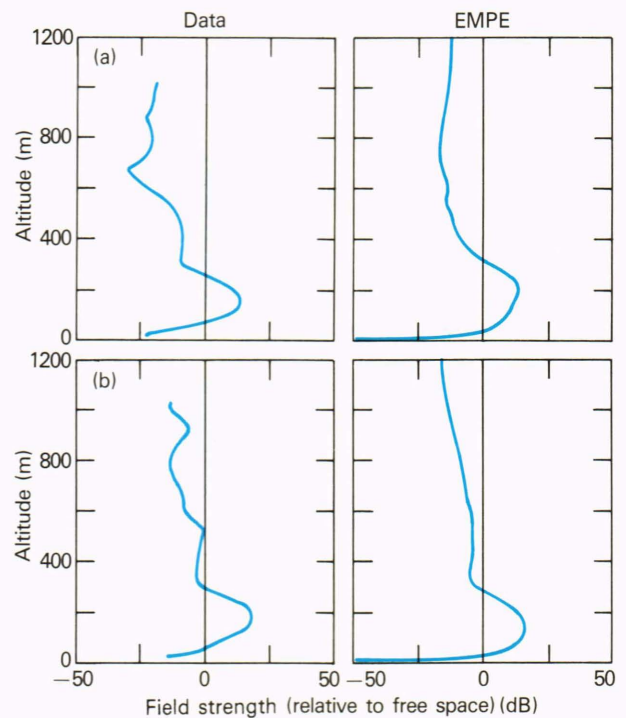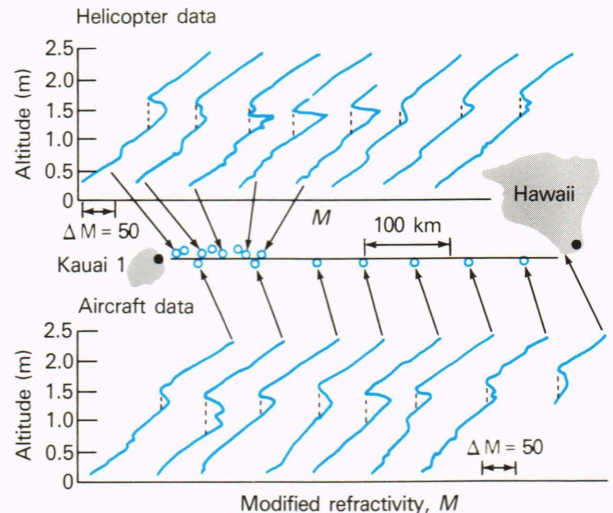
age above the duct. Figure 14b shows the coverage predicted for the same antenna in the laterally inhomogeneous, elevated-duct environment shown in Fig. 13. Here, there is great duct leakage and complex mode structure, especially between the ranges of 400 and 500 km.

Figure 15a compares the EMPE prediction with data obtained by the UH-3 helicopter on 22 June 1977. This is a vertical loss plot in which the transmitter–receiver range is held constant at 480 km. The comparison clearly shows the inadequacy of the assumption of lateral ho-
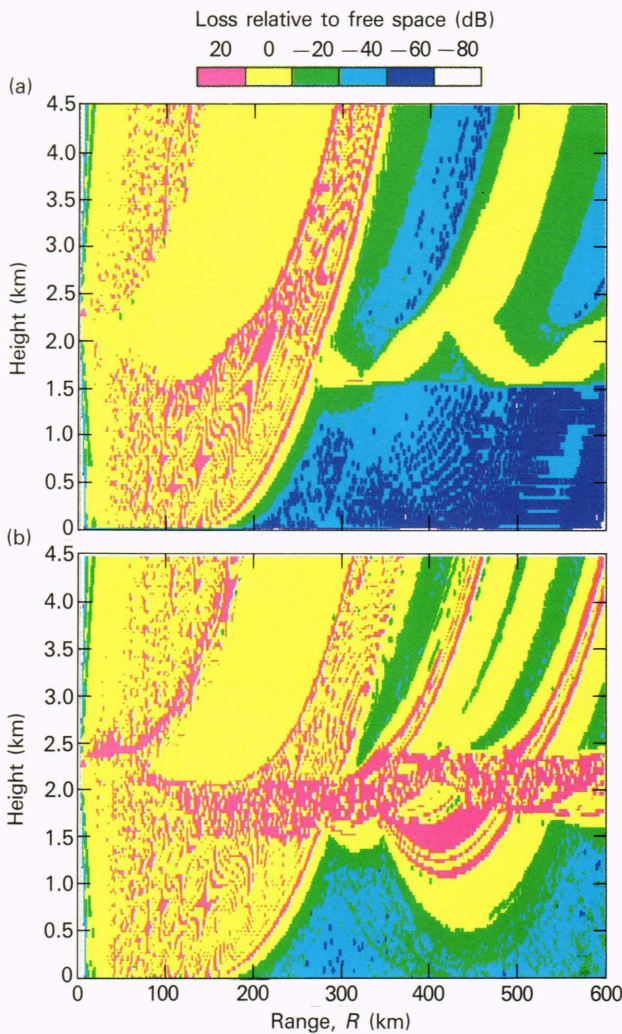
Figure 14—EMPE coverage diagrams for elevated-duct activity off Hawaii on 22 June 1977 for (a) horizontally homogeneous duct average features and (b) laterally inhomogeneous, range-dependent profiles given by Fig. 13. Transmitter frequency of 2.2 GHz, with an antenna height of 1554 m.

Figure 15—Comparison between EMPE (dark) and elevated-duct (light) data obtained off Hawaii on 22 June 1977 for (a) horizontally homogeneous duct average features and constant range, and (b) horizontally inhomogeneous actual duct profiles and increasing range during descent.

mogeneity to describe the data. Figure 15b tries to match the description of the measurement by using EMPE results that are obtained for the UH-3 track, which is descending and increasing in range from 465 to 493 km from the transmitter. Note that there is more energy predicted by EMPE than measured at the lower altitude. Examination of Fig. 14b shows that moving the UH-3 track nearer to the transmitter by only 20 km would reduce the EMPE energy considerably beneath the elevated duct. In fact, there is an uncertainty of 25 km in the lateral range of the transmitter on board the UH-1 helicopter because of its orbiting status, illustrating the need for adequate experimental control of transmitter–receiver track and reconstructive information. Many other published datasets have not been analyzed, because of the lack of such experimental controls and of computational ability, particularly in the gigahertz range of frequencies. Fortunately, the advent of EMPE is stimulating further experiments of quality.[3]
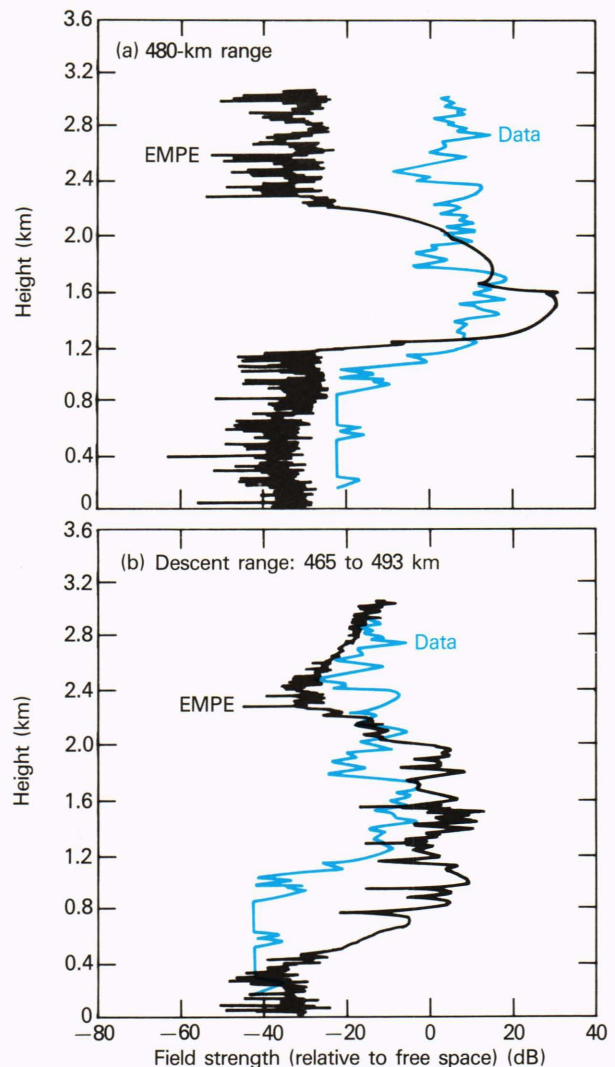
SUMMARY

Since the original articles in this publication describing the EMPE model, the model has been validated repeatedly against both measured and modeled losses. Calculations made with EMPE are helping to explain radar and communications observations that previously could not be easily understood. APL investigators are routinely predicting antenna coverage for sites worldwide because of the assurance that, within the constraints imposed by its formulation, EMPE provides useful estimates for propagation loss in most anomalous environments.

The comparisons of EMPE results with measured losses have yielded good agreement in many cases, although experimental data and controls have not been adequate for precise analysis by any code. The chief advantages of EMPE over other models are its efficiency and its

ability to handle complex, varying refractivity environments. For the gigahertz frequencies of current interest, EMPE is orders of magnitude faster than the established models based on mode theory, and it agrees well with these models on classical test cases.

REFERENCES

[1] H. W. Ko, J. W. Sari, and J. P. Skura, "Anomalous Microwave Propagation Through Atmospheric Ducts," *Johns Hopkins APL Tech. Dig.* **4**, 12–26 (1983).

[2] C. E. Schemm, L. P. Manzi, and H. W. Ko, "A Predictive System for Estimating the Effects of Range- and Time-Dependent Anomalous Refraction on Electromagnetic Wave Propagation," *Johns Hopkins APL Tech. Dig.* **8**, 394–403 (1987).

[3] G. D. Dockery and G. C. Konstanzer, "Recent Advances in the Prediction of Tropospheric Propagation Using the Parabolic Equation," *Johns Hopkins APL Tech. Dig.* **8**, 404–412 (1987).

[4] H. W. Ko, "Anomalous Propagation Effects on Microwave Systems," *IEEE Electro 86* **E27**, pp. 1–21 (1986).

[5] J. P. Skura, "Worldwide Anomalous Refraction and its Effects on Electromagnetic Wave Propagation," *Johns Hopkins APL Tech. Dig.* **8**, 418–425 (1987).

[6] S. H. Cho and J. R. Wait, "Analysis of Microwave Ducting in an Inhomogeneous Troposphere," *Pure Appl. Geophys.* **116**, 1118–1142 (1978).

[7] V. Fock, "Solution of the Problem of Propagation of Electromagnetic Waves Along the Earth's Surface by the Method of Parabolic Equation," *J. Phys. of U.S.S.R.* **10**, 13–35, (1946).

[8] M. A. Leontovich, "On the Approximate Boundary Conditions for an Electromagnetic Field on the Surface of Well-Conducting Bodies," Chap. in *Investigation of Propagation of Radio Waves,* B. A. Vedensky, ed., Academy of Science, Moscow (1948).

[9] R. R. Pappert, *Case Study of Propagation in a Laterally Inhomogeneous Duct in the Lower and Mid VHF Band,* NOSC TN1119, Naval Ocean Systems Center (1982).

[10] D. E. Kerr, *Propagation of Short Radio Waves,* McGraw-Hill, N.Y., 382–385 (1951).

[11] M. Katzin, R. Bauchman, and W. Binnian, "3 and 9 Centimeter Propagation in Low-Ocean Ducts," *Proc. IRE* **35**, 891–905 (1947).

[12] C. L. Pekeris, "Wave Theoretical Interpretation of Propagation of 10-cm and 3-cm Waves in Low Level Ocean Ducts," *Proc. IRE* **35**, 453–462 (1947).

[13] H. V. Hitney, J. R. Richter, R. A. Pappert, K. D. Anderson, and G. B. Baumgartner, "Tropospheric Radio Propagation Assessment," *Proc. IEEE* **73**, 265–283 (1985).

[14] L. G. Trolese, "Tropospheric Propagation Characteristics," in *Symp. Tropospheric Wave Propagation,* NEL TR173, pp. 17–61 (1949).

[15] J. L. Skillman and D. R. Woods, *Experimental Study of Elevated Ducts,* NOSC TD260, Naval Ocean Systems Center, pp. 93–106 (1979).

THE AUTHORS
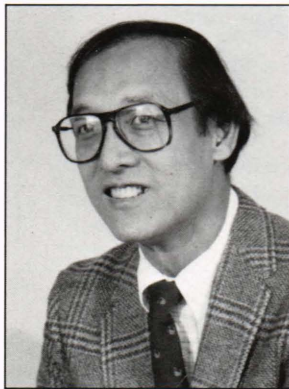
HARVEY W. KO was born in Philadelphia in 1944 and received the B.S.E.E. (1967) and Ph.D. (1973) degrees from Drexel University. During 1964–65, he designed communications trunk lines for the Bell Telephone Company. In 1966, he performed animal experiments and spectral analysis of pulsatile blood flow at the University of Pennsylvania Presbyterian Medical Center.

After joining APL in 1973, he investigated analytical and experimental aspects of ocean electromagnetics, including ELF wave propagation and magnetohydrodynamics. Since 1981, he has been examining radar wave propagation in coastal environments, advanced biomagnetic processing for encephalography, and brain edema. He is now a member of the Submarine Technology Department staff.
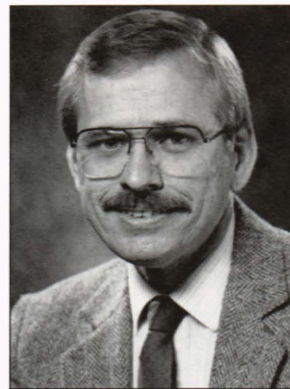
JOSEPH P. SKURA was born in Mineola, N.Y., in 1952 and received the M.S. degree in applied physics from Adelphi University (1976). During 1974–75, he performed research on the reverse eutrophication of lakes for Union Carbide. During 1975–78, he performed research on the combustion of coal–oil–water slurries for the Department of Transportation, New England Power and Light Co., and NASA.

After joining APL's Submarine Technology Department in 1978, Mr. Skura investigated ocean electromagnetics, including ELF wave propagation. Since 1981, he has been examining radar-wave propagation under anomalous propagation conditions. In 1986, he became involved in several biomedical projects, including bone healing, epilepsy, and brain edema.
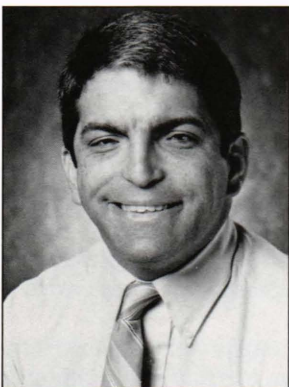
HOWARD S. BURKOM was born in Baltimore in 1948. He received a B.A. in mathematics from Lehigh University in 1970. In 1975 he completed his Ph.D. in geometric topology at the University of Illinois, Urbana. He was an Assistant Professor at Southern Illinois University until 1976. For the past nine years, Dr. Burkom has worked for Sachs/Freeman Associates at APL, principally in the modeling and analysis of propagation loss. He has dealt with a variety of problems in underwater acoustics and in system design and guidance for the Environmental and Acoustic Groups. Since 1986 he has also been studying electromagnetic propagation in the troposphere through his work on the theoretical aspects and validation of the EMPE model.
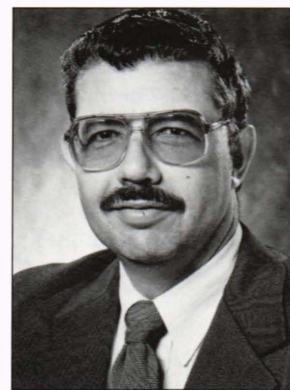
DURVIS A. ROBERTS was born in San Angelo, Tex., in 1943. He received a B.E.S. degree from the University of Texas in 1967 and M.S. degrees in space technology (1977) and computer science (1979) from The Johns Hopkins University. Since joining Sachs/Freeman Associates, he has provided analysis and programming support to APL's Strategic Systems (1974–77) and Submarine Technology (1977–present) Departments. He has been involved in systems simulation, real-time data acquisition systems development, and analysis software for ocean experiments. Since 1985 Mr. Roberts has been examining the effects of electromagnetic wave propagation under anomalous propagation conditions.